

Universität des Saarlandes



Fachrichtung 6.1 – Mathematik

Preprint Nr. 336

**Arbitrary order BEM-based Finite Element
Method on polygonal meshes**

Steffen Weißer

Saarbrücken 2013

Arbitrary order BEM-based Finite Element Method on polygonal meshes

Steffen Weißer

Saarland University
Department of Mathematics
P.O. Box 15 11 50
66041 Saarbrücken
Germany
weisser@num.uni-sb.de

Edited by
FR 6.1 – Mathematik
Universität des Saarlandes
Postfach 15 11 50
66041 Saarbrücken
Germany

Fax: + 49 681 302 4443
e-Mail: preprint@math.uni-sb.de
WWW: <http://www.math.uni-sb.de/>

Arbitrary order BEM-based Finite Element Method on polygonal meshes

Steffen Weißer

September 20, 2013

Abstract

Polygonal meshes show up in more and more applications and the BEM-based Finite Element Method turned out to be a forward-looking approach. The method uses implicitly defined trial functions, which are treated locally by means of Boundary Element Methods (BEM). Due to this choice the BEM-based FEM is applicable on a variety of meshes including hanging nodes. The aim of this presentation is to give a rigorous construction of H^1 -conforming trial functions yielding arbitrary order of convergence in a Finite Element Method for elliptic equations. With the help of an interpolation operator, approximation properties are proven which guaranty optimal rates of convergence in the H^1 - as well as in the L_2 -norm for FEM simulations. These theoretical results are illustrated and verified by several numerical examples on polygonal meshes.

Keywords BEM-based FEM · polygonal finite elements · convergence estimates · polygonal mesh · non-standard finite element method

Mathematics Subject Classification (2000) 65N30 · 65N38 · 41A25 · 41A30

1 Introduction

Physical models and computer simulations play a crucial role in the development and research of almost all areas. Lots of them rely on boundary value problems in their mathematical formulations. Thus, an efficient and flexible numerical treatment of such differential equations with boundary conditions is of particular interest. The Finite Element Method (FEM) is one of the favourite strategies which makes use of a discretization of the domain into simple elements like triangles, quadrangles (2D) or tetrahedra (3D), for example. However, in nowadays application which appear in geological science, solid mechanics, biomechanics and fluid dynamics, there is a need for more flexible methods. The discretization of complex domains might yield unstable meshes using solely simple elements.

The present investigation extends the theory [28] of a special Finite Element Method, called BEM-based FEM, which is applicable on general polygonal meshes due to the use of local Boundary Element Methods (BEM). The restriction of convex elements is loosened and a conforming approximation space is introduced which yields arbitrary order of convergence. With the help of an appropriate interpolation operator, approximation estimates are proven in the H^1 - as well as in the L_2 -norm. These results are similar to standard Finite Element Methods but on much more general meshes.

The BEM-based FEM was first introduced in 2009, see [9], and analysed in the following years, see [10, 14, 16, 24]. Since then it has undergone several developments. This includes residual error estimates for adaptive mesh refinement [31], the application for convection–diffusion problems [17] and mixed formulations with $H(\text{div})$ -conforming discretizations [11] as well as improved generalizations to three dimensional problems with polyhedral elements [27]. The main results have been gathered in two doctoral theses [15, 32].

In the case of a diffusion problem, the lowest order trial functions coincide with harmonic coordinates studied and applied in computer graphics, see [19, 21]. These functions belong to the class of generalized barycentric coordinates which are constructed over polygonal elements. An analysis can be found in [12] and there are even the first attempts to define quadratic conforming functions on polygons [25]. Such functions are also applied in linear elasticity [30], for example. Beside the Finite Element Method there are also other strategies for the numerical approximation of boundary value problems. In the context of polygonal meshes and conforming approximations there are recent developments in mimetic discretization techniques [5] and within the new methodology of Virtual Element Methods [3, 4, 2].

The paper is organized as follows. In Section 2, the model problem is introduced, and the regularity as well as stability assumptions for polygonal meshes are discussed. In Section 3, we give the definition of the basis functions for the construction of the H^1 -conforming approximation space. Furthermore, interpolation operators are introduced and their properties are proven. In Section 4, we formulate and discuss the BEM-based Finite Element Method with the introduced approximation space and give convergence estimates. These convergence rates are confirmed by numerical experiments in Section 5. Finally, we conclude our results in Section 6.

2 Preliminaries

The approximation space in the BEM-based FEM is defined in accordance with the underlying differential equation of the considered boundary value problem. For this presentation, we choose the diffusion problem with mixed boundary conditions on a bounded polygonal domain $\Omega \subset \mathbb{R}^2$. Its boundary $\Gamma = \Gamma_D \cup \Gamma_N$

is split into a Dirichlet and a Neumann part, where we assume $|\Gamma_D| > 0$. For a given source term $f \in L_2(\Omega)$, a Dirichlet datum $g_D \in H^{1/2}(\Gamma_D)$ as well as a Neumann datum $g_N \in L_2(\Gamma_N)$, the problem reads

$$\begin{aligned} -\operatorname{div}(a\nabla u) &= f && \text{in } \Omega, \\ u &= g_D && \text{on } \Gamma_D, \\ a\nabla u \cdot n &= g_N && \text{on } \Gamma_N, \end{aligned} \tag{1}$$

where $a \in L_\infty(\Omega)$ with $0 < a_{\min} \leq a \leq a_{\max}$ almost everywhere in Ω . This boundary value problem is considered in the weak sense with the help of a Galerkin formulation. Thus, we seek a solution $u \in H^1(\Omega)$, where we denote as usual the Sobolev spaces of order $s \in \mathbb{R}$ with $H^s(D)$ for some domain $D \subset \Omega$, see [1, 22]. For simplicity, we assume that the diffusion coefficient a is piecewise constant and its jumps are resolved by the meshes later on. Nevertheless, we will also give a hint for the more general case. Our goal is to introduce a H^1 -conforming approximation space which yields arbitrary order of convergence in the finite element framework. The following discrete approximation of $H^1(\Omega)$ is constructed but not limited to the diffusion equation. It also can be applied to other boundary value problems where H^1 -conforming approximations are desirable.

One of the major advantages of the BEM-based FEM is the flexibility with respect to the discretization of Ω , which is needed in the Finite Element Method. Consider for $h \rightarrow 0$ a family of discretizations \mathcal{K}_h . For fixed h , a discretization is obtained by decomposing Ω into a finite number of elements. The elements $K \in \mathcal{K}_h$ of the mesh are bounded open sets of polygonal shape which are non-overlapping such that $\bar{\Omega} = \bigcup \{x \in \bar{\Omega} : K \in \mathcal{K}_h\}$. Their boundaries ∂K consist of finitely many nodes and edges. An edge $E = \overline{z_b z_e}$ is always located between two nodes, the one at the beginning z_b and the one at the end z_e . These points are fixed once per edge and they are the only nodes on E . The set of all edges in the mesh is denoted by \mathcal{E}_h . In each corner of an element K , a node is located, but there could also be nodes on straight lines of the boundary ∂K . This behaviour is natural to polygonal meshes and relaxes the regularity assumptions for usual triangular and quadrangular meshes, where such nodes have to be treated in a special way as conditional nodes. The set of all nodes in the mesh is abbreviated to \mathcal{N}_h . The length of an edge E and the diameter of an element K are denoted by h_E and $h_K = \sup\{|x - y| : x, y \in \partial K\}$, respectively.

Definition 1. The family of meshes \mathcal{K}_h is called regular if it fulfills:

1. Each element $K \in \mathcal{K}_h$ is a star-shaped polygon with respect to a circle of radius ρ_K and midpoint z_K .
2. The aspect ratio is uniformly bounded from above by $\sigma_{\mathcal{K}}$, i.e. $h_K/\rho_K < \sigma_{\mathcal{K}} \quad \forall K \in \mathcal{K}_h$.

The circle in the definition is chosen in such a way that its radius is maximal. If the position of the circle is not unique, its midpoint z_K is fixed once per element.

Definition 2. The family of meshes \mathcal{K}_h is called stable if there is a constant $c_{\mathcal{K}} > 0$ such that for all elements $K \in \mathcal{K}_h$ and all its edges $E \subset \partial K$ it holds

$$h_K \leq c_{\mathcal{K}} h_E.$$

When we consider convergence or error estimates with respect to the mesh size $h = \max\{h_K : K \in \mathcal{K}_h\}$, it is important that the constants in the definitions above hold uniformly for the whole family of meshes. For convenience we only write mesh in the following and mean a whole family for $h \rightarrow 0$. Furthermore, we denote by c a generic constant which solely depends on the mesh constants and which is especially independent of h . Without loss of generality, we assume $h < 1$ that can always be satisfied by scaling of the domain. Later on, we need the space of polynomials of degree smaller or equal $k \in \mathbb{N}$ over some domain $D \subset \Omega$. This space is abbreviated to $\mathcal{P}^k(D)$. For a vector space V with subspace V_0 , we set for $v \in V$ the affine space

$$v + V_0 = \{v + v_0 \in V : v_0 \in V_0\}.$$

3 Discretization and interpolation

Our goal is to introduce finite dimensional spaces V_h^q over polygonal discretizations of the domain Ω which approximate the Sobolev space $H^1(\Omega)$. The index $q \in \mathbb{N}$ denotes the order of the approximation space. In [28], the cases $q = 1, 2$ are already studied. In this section, we give a more general strategy which extends the theory to arbitrary order. The approximation space $V_h^q = \text{span } \Psi_h^q$ is constructed as span of some basis Ψ_h^q . This basis is specified in the following and consists of nodal, edge and element basis functions. These functions are indicated by ψ_z , ψ_E and ψ_K , respectively. All of them have certain degrees and thus they are marked and numbered by indices like $\psi_{E,i}$ and $\psi_{K,i,j}$ for some i, j . However, for shorter notation, we will skip sometimes parts of the indices if the meaning is clear from the context and we just write ψ , ψ_i and $\psi_{i,j}$, for example.

The basis functions are defined implicitly element-by-element with the help of local boundary value problems. The diffusion equation in mind, we utilize Laplace and Poisson equations over each element with Dirichlet boundary data to construct the basis functions. Due to the local Dirichlet boundary conditions, the traces of the basis functions will be continuous over element boundaries. This is an essential ingredient to obtain H^1 -conforming approximations.

3.1 Node and edge basis functions

The functions ψ_z and ψ_E , which are assigned to nodes and edges, are defined to fulfill the Laplace equation on each element. Their Dirichlet trace on the element

boundaries is chosen to be continuous and piecewise polynomial. Thus, we define for each node $z \in \mathcal{N}_h$ the basis function ψ_z as usual, see [28, 31], namely as unique solution of

$$-\Delta\psi_z = 0 \quad \text{in } K \quad \text{for all } K \in \mathcal{K}_h,$$

$$\psi_z(x) = \begin{cases} 1 & \text{for } x = z \\ 0 & \text{for } x \in \mathcal{N}_h \setminus \{z\} \end{cases},$$

ψ_z is linear on each edge of the mesh.

So, the function ψ_z is locally defined as solution of a boundary value problem over each element. If the element $K \in \mathcal{K}_h$ is convex, the boundary value problem can be understood in the classical sense and it is $\psi_z \in C^2(K) \cap C^0(\overline{K})$, see [13]. However, we explicitly allow star-shaped elements within the discretization \mathcal{K}_h of the domain Ω . In this case, the boundary value problem is understood in the weak sense and we obtain $\psi_z \in H^1(K)$. Since the Dirichlet trace on the element boundaries is continuous, the local regularity of ψ_z yields $\psi_z \in H^1(\Omega)$. This will be also true for the edge and element basis functions. In the following, the local problems for the definition of basis functions are always understood in the classical or weak sense depending on the shape of the elements. In contrast to [28], we only make use of the fact that the nodal, edge and element basis functions fulfill $\psi \in H^1(K)$ for $K \in \mathcal{K}_h$ and we do not use a maximum-principle for harmonic functions which would require convex elements.

To introduce the edge basis functions ψ_E , polynomial data is prescribed on the element boundaries. Therefore, we first review a hierarchical polynomial basis over the interval $[0, 1]$. We set

$$p_0(t) = t \quad \text{and} \quad p_1(t) = 1 - t$$

for $t \in [0, 1]$ and assign these functions to the points $t_0 = 0$ and $t_1 = 1$, respectively. Then, we define $p_i \in \mathcal{P}^i([0, 1])$, $i \geq 2$ with exact degree i recursively as

$$p_i = \frac{\tilde{p}_i}{\tilde{p}_i(t_i)},$$

where $\tilde{p}_i \in \mathcal{P}^i([0, 1]) \setminus \{0\}$ is a polynomial with $\tilde{p}_i(t_j) = 0$ for $j = 0, \dots, i-1$ and

$$t_i = \max\{\arg \max_{t \in [0, 1]} |\tilde{p}_i(t)|\}.$$

The polynomial p_i is well defined since \tilde{p}_i is unique up to a multiplicative constant. In Figure 1, the first polynomials are visualized. It is easily seen that these polynomials are linearly independent and that for $q \geq 1$

$$\mathcal{P}^q([0, 1]) = \text{span} \{p_i : i = 0, \dots, q\}.$$

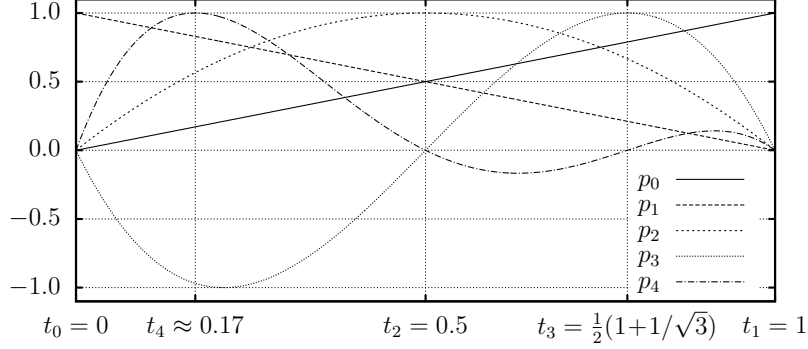


Figure 1: Visualization of p_i for $i = 0, \dots, 4$

For the definition of edge basis functions ψ_E , we make use of a linear parametrization of the corresponding edge. Let $E \in \mathcal{E}_h$ with $E = \overline{z_b z_e}$ and

$$E : [0, 1] \ni t \mapsto F_E(t) = z_b + t(z_e - z_b).$$

In contrast to nodal basis functions, we have more than one basis function per edge. We define $\psi_{E,i}$ for $i = 2, \dots, q$ as unique solution of

$$\begin{aligned} -\Delta \psi_{E,i} &= 0 \quad \text{in } K \quad \text{for all } K \in \mathcal{K}_h, \\ \psi_{E,i} &= \begin{cases} p_i \circ F_E^{-1} & \text{on } E, \\ 0 & \text{on } \mathcal{E}_h \setminus \{E\}, \end{cases} \end{aligned}$$

and we assign these functions to the points $z_{E,i} = F_E(t_i)$. In Figure 2, an approximation of such a function is visualized over one rectangular element. As in the case of nodal basis functions, we observe that the Dirichlet trace is continuous along element boundaries. Thus, we have $\psi_{E,i} \in H^1(K)$ for $K \in \mathcal{K}_h$ which yields $\psi_{E,i} \in H^1(\Omega)$. With the conventions

$$\psi_{E,0} = \psi_{z_b} \quad \text{and} \quad \psi_{E,1} = \psi_{z_e},$$

we find that

$$\mathcal{P}^q(E) = \text{span} \{ \psi_{E,i}|_E : i = 0, \dots, q \}$$

and

$$\psi_{E,i}(z_{E,j}) = \delta_{ij} \quad \text{for } j = 0, \dots, i,$$

where δ_{ij} is the Kronecker symbol. According to the last property, the functions ψ_z and $\psi_{E,i}$ are linearly independent. So, we collect them in the basis

$$\Psi_{h,\partial}^q = \{ \psi_z, \psi_{E,i} : z \in \mathcal{N}_h, E \in \mathcal{E}_h, i = 2, \dots, q \},$$

and we have

$$V_{h,\partial}^q = \text{span } \Psi_{h,\partial}^q \subset H_{\Delta}^1(\mathcal{K}_h) \subset H^1(\Omega).$$

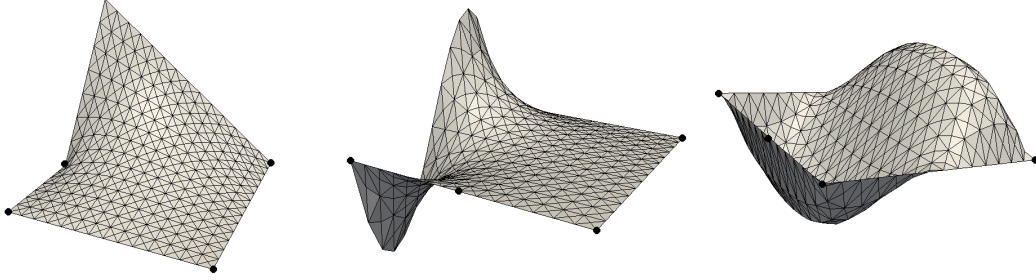


Figure 2: Visualization of ψ_z , $\psi_{E,3}$ and $\psi_{K,1,0}$ over rectangular element with additional node on straight line, nodes are marked with black dots

Here, for $q = 1$, only nodal basis functions are used in $\Psi_{h,\partial}^q$ and for $k \in \mathbb{N}$,

$$H_{\Delta}^k(\mathcal{K}_h) = \{v \in H^k(\Omega) : (\nabla v, \nabla w)_{L_2(K)} = 0 \quad \forall w \in H_0^1(K), \forall K \in \mathcal{K}_h\} \quad (2)$$

is the space of piecewise weakly harmonic functions.

3.2 Element basis functions

Next, we address the definition of element basis functions. To motivate the procedure, we remember that the nodal and edge basis functions fulfill the Laplace equation inside the elements and are polynomial on the edges. The nodal functions are linear on edges, and thus we conclude that these functions also fulfill the one dimensional Laplace equation along edges. If we compute the 1D-Laplacian of the edge functions ψ_E along the edge E , we observe that $\Delta_1 \psi_{E,i} \in \mathcal{P}^{i-2}(E)$, $i \geq 2$, and thus the edge basis functions fulfill the Poisson equation with polynomial right hand side on each edge. Additionally, it is easy to check that

$$\mathcal{P}^{q-2}(E) = \text{span} \{\Delta_1 \psi_{E,i} : i = 2, \dots, q\}$$

for $q \geq 2$. From this point of view, we exchanged the Laplace equation for the Poisson equation on the edges as we have made the step from nodal to edge basis functions. The same is done for the element basis functions. Here, we exchange the Laplace for the Poisson equation in the elements and we prescribe right hand sides such that they form a basis of $\mathcal{P}^{q-2}(K)$. Thus, we define $\psi_{K,i,j}$ for $K \in \mathcal{K}_h$, $i = 0, \dots, q-2$ and $j = 0, \dots, i$ as unique solution of

$$\begin{aligned} -\Delta \psi_{K,i,j} &= p_{K,i,j} && \text{in } K, \\ \psi_{K,i,j} &= 0 && \text{else,} \end{aligned} \quad (3)$$

where

$$\mathcal{P}^{q-2}(K) = \text{span} \{p_{K,i,j} : i = 0, \dots, q-2 \text{ and } j = 0, \dots, i\}. \quad (4)$$

Consequently, we have $\frac{1}{2}q(q-1)$ element basis functions per element. The support of such a function is limited to one element, i.e. $\text{supp } \psi_{K,i,j} = \overline{K}$, and the function

itself belongs to $H_0^1(K)$. Due to the local regularity, we obtain $\psi_{K,i,j} \in H^1(\Omega)$. See Figure 2 for a visualization of such an element basis function.

Remark 1. In the numerical experiments we will choose the polynomial basis as shifted monomials, namely as

$$p_{K,i,j}(x) = \left(x^{(1)} - z_K^{(1)}\right)^{i-j} \left(x^{(2)} - z_K^{(2)}\right)^j, \quad x = \left(x^{(1)}, x^{(2)}\right)^\top \in K,$$

where $z_K = \left(z_K^{(1)}, z_K^{(2)}\right)^\top$ is given in Definition 1. For $i, j = 0$, the element bubble function from [28] is recovered, since $p_{K,0,0} = 1$.

We define the set of functions

$$\Psi_{h,\circ}^q = \{\psi_{K,i,j} : K \in \mathcal{K}_h, i = 0, \dots, q-2 \text{ and } j = 0, \dots, i\}$$

and the space

$$V_{h,\circ}^q = \text{span } \Psi_{h,\circ}^q \subset H^1(\Omega).$$

For $q = 1$, this means $\Psi_{h,\circ}^q = \emptyset$. Furthermore, we point out that each $\psi_{K,i,j} \in \Psi_{h,\circ}^q$ fulfills

$$\left(\nabla \psi_{K,i,j}, \nabla w\right)_{L_2(K)} = \left(p_{K,i,j}, w\right)_{L_2(K)} \quad \forall w \in H_0^1(K) \quad (5)$$

according to its definition.

Lemma 1. *The functions in $\Psi_{h,\circ}^q$ are linearly independent.*

Proof. Since the support of an element basis function is restricted to one element, the functions belonging to different elements are independent. Therefore, it is sufficient to consider just functions over one element in this proof. Let $\alpha_{i,j} \in \mathbb{R}$ for $i = 0, \dots, q-2$ and $j = 0, \dots, i$ and let $\sum_{i,j} \alpha_{i,j} \psi_{i,j} = 0$. Consequently, it is $\sum_{i,j} \alpha_{i,j} \nabla \psi_{i,j} = 0$. Due to this and since the element basis functions $\psi_{i,j} = \psi_{K,i,j}$ fulfill (5), we obtain

$$\left(\sum_{i,j} \alpha_{i,j} p_{i,j}, w\right)_{L_2(K)} = \left(\sum_{i,j} \alpha_{i,j} \nabla \psi_{i,j}, \nabla w\right)_{L_2(K)} = 0 \quad \forall w \in H_0^1(K).$$

The function space $C_0^\infty(K)$ is dense in $H_0^1(K)$ and thus the fundamental lemma of the calculus of variations yields $\sum_{i,j} \alpha_{i,j} p_{i,j} = 0$. Because of the choice of $p_{i,j}$ as basis of $\mathcal{P}^{q-2}(K)$, it follows that $\alpha_{i,j} = 0$ for $i = 0, \dots, q-2$ and $j = 0, \dots, i$. \square

The final basis for the approximation space of $H^1(\Omega)$ is now defined as

$$\Psi_h^q = \Psi_{h,\partial}^q \cup \Psi_{h,\circ}^q.$$

All functions in $\Psi_{h,\partial}^q$ locally fulfill the Laplace equation on each element and so, they are piecewise harmonic in a weak sense. Therefore, the functions in $\Psi_{h,\circ}^q$ serve complementary to those in $\Psi_{h,\partial}^q$ such that functions in $H^1(\Omega)$, which are

not locally harmonic, can be approximated in an accurate way. Furthermore, we observe that

$$(\nabla\psi, \nabla\varphi)_{L_2(K)} = 0 \quad \text{for } \psi \in \Psi_{h,\partial}^q, \varphi \in \Psi_{h,\circ}^q, \quad (6)$$

since $\psi \in H_{\Delta}^1(\mathcal{K}_h)$ and $\varphi \in H_0^1(K)$, cf. (2). Sometimes, we will consider the basis functions restricted to one element. For this reason, we define for $K \in \mathcal{K}_h$

$$\Psi_h^q|_K = \{\psi|_K : \psi \in \Psi_h^q\}$$

and $\Psi_{h,\partial}^q|_K$ as well as $\Psi_{h,\circ}^q|_K$ accordingly. The final approximation space is conforming, i.e.

$$V_h^q = \text{span } \Psi_h^q \subset H^1(\Omega).$$

3.3 Interpolation and properties

Next, some interpolation operators are introduced. The first one is a pointwise interpolation operator

$$\mathfrak{I}_{h,\partial}^q : H^2(\Omega) \rightarrow V_{h,\partial}^q \subset H_{\Delta}^1(\mathcal{K}_h).$$

For $v \in H^2(\Omega)$, it is

$$\mathfrak{I}_{h,\partial}^q v = \sum_{z \in \mathcal{N}_h} v_z \psi_z + \sum_{E \in \mathcal{E}_h} \sum_{i=2}^q v_{E,i} \psi_{E,i},$$

where the coefficients are given as

$$v_z = v(z) \quad \text{for } z \in \mathcal{N}_h$$

and

$$v_{E,i} = v(z_{E,i}) - \sum_{j=0}^{i-1} v_{E,j} \psi_{E,j}(z_{E,i}) \quad \text{for } E \in \mathcal{E}_h, i = 2, \dots, q.$$

The pointwise evaluation of the function $v \in H^2(\Omega)$ is well defined according to the Sobolev embedding theorem, see [1], which states that $v \in C^0(\overline{\Omega})$. The interpolation operator is constructed in such a way that

$$\begin{aligned} (\mathfrak{I}_{h,\partial}^q v)(z) &= v(z) \quad \text{for } z \in \mathcal{N}_h, \\ (\mathfrak{I}_{h,\partial}^q v)(z_{E,i}) &= v(z_{E,i}) \quad \text{for } E \in \mathcal{E}_h, i = 2, \dots, q. \end{aligned} \quad (7)$$

Furthermore, we introduce the interpolation operator

$$\mathfrak{I}_h^q = \mathfrak{I}_{h,\partial}^q + \mathfrak{I}_{h,\circ}^q : H^2(\Omega) \rightarrow V_h^q \subset H^1(\Omega),$$

where

$$\mathfrak{I}_{h,\circ}^q v = \sum_{K \in \mathcal{K}_h} \sum_{i=0}^{q-2} \sum_{j=0}^i v_{K,i,j} \psi_{K,i,j} \in V_{h,\circ}^q.$$

Since element basis functions, which belong to different elements, have non-overlapping support, the coefficients of the linear combination can be specified element-by-element. Let $K \in \mathcal{K}_h$, the coefficients $v_{i,j} = v_{K,i,j}$ are defined such that $\mathfrak{I}_{h,\circ}^q v$ is the orthogonal projection of $v - \mathfrak{I}_{h,\partial}^q v$ into $\text{span } \Psi_{h,\circ}^q|_K$ with respect to the weighted scalar product

$$(u, v)_{hH^1(K)} = (u, v)_{L_2(K)} + h_K^2 (\nabla u, \nabla v)_{L_2(K)}. \quad (8)$$

Thus, $\mathfrak{I}_{h,\circ}^q v$ is uniquely defined by

$$(\mathfrak{I}_{h,\circ}^q v, \varphi)_{hH^1(K)} = (v - \mathfrak{I}_{h,\partial}^q v, \varphi)_{hH^1(K)} \quad \forall \varphi \in \text{span } \Psi_{h,\circ}^q|_K. \quad (9)$$

Due to the properties of the orthogonal projection, it is

$$\|\mathfrak{I}_{h,\circ}^q v\|_{hH^1(K)} \leq \|v - \mathfrak{I}_{h,\partial}^q v\|_{hH^1(K)}, \quad (10)$$

where the weighted norm is given as $\|\cdot\|_{hH^1(K)}^2 = (\cdot, \cdot)_{hH^1(K)}$. If $h_K = 1$ the weighted scalar product and the weighted norm coincide with the usual ones in $H^1(K)$, which are denoted by $(\cdot, \cdot)_{H^1(K)}$ and $\|\cdot\|_{H^1(K)}$, respectively.

In the following, we investigate the properties of the interpolation operators in more details. For this reason, let \mathcal{K}_h be a regular and stable mesh. We denote the interpolation operator restricted to some element $K \in \mathcal{K}_h$ by the same symbol as the global one since the meaning is clear from the context.

Lemma 2. *The restrictions of the interpolation operators $\mathfrak{I}_{h,\partial}^q$ and \mathfrak{I}_h^q onto an element $K \in \mathcal{K}_h$ fulfill*

$$\mathfrak{I}_{h,\partial}^q p = p \quad \text{for } p \in \mathcal{P}^q(K) \text{ with } \Delta p = 0 \text{ in } K,$$

and

$$\mathfrak{I}_h^q p = p \quad \text{for } p \in \mathcal{P}^q(K).$$

Proof. Let $p \in \mathcal{P}^q(K)$ with $\Delta p = 0$. According to (7), the functions p and $\mathfrak{I}_{h,\partial}^q p$ coincide in $q + 1$ points on each edge of the element K and they are both polynomials of degree q along these edges. Thus, p and $\mathfrak{I}_{h,\partial}^q p$ are identical on the boundary of the element K . Furthermore, both functions fulfill the Laplace equation inside K . Thus, the unique solvability of the Dirichlet problem for the Laplace equation yields $\mathfrak{I}_{h,\partial}^q p = p$, the first statement of the lemma.

Next, let $p \in \mathcal{P}^q(K)$ and therefore it is $-\Delta p \in \mathcal{P}^{q-2}(K)$. Since the polynomials $p_{i,j}$ form a basis of $\mathcal{P}^{q-2}(K)$, see (4), we can write

$$-\Delta p = \sum_{i=0}^{q-2} \sum_{j=0}^i \beta_{i,j} p_{i,j}$$

for some uniquely chosen coefficients $\beta_{i,j} \in \mathbb{R}$. Furthermore, we define

$$\tilde{p} = \mathfrak{I}_{h,\partial}^q p + \sum_{i=0}^{q-2} \sum_{j=0}^i \beta_{i,j} \psi_{i,j}. \quad (11)$$

We observe that p as well as \tilde{p} fulfill the boundary value problem

$$\begin{aligned} -\Delta u &= \sum_{i=0}^{q-2} \sum_{j=0}^i \beta_{i,j} p_{i,j} \quad \text{in } K, \\ u &= p \quad \text{on } \partial K, \end{aligned}$$

at least in the weak sense, due to construction. Because of the unique solvability of this problem, we conclude that $p = \tilde{p}$. In consequence of (11), we obtain

$$p - \mathfrak{I}_{h,\partial}^q p = \sum_{i=0}^{q-2} \sum_{j=0}^i \beta_{i,j} \psi_{i,j} \in \text{span } \Psi_{h,\circ}^q|_K.$$

Since $\mathfrak{I}_{h,\circ}^q p$ is defined as orthogonal projection of $p - \mathfrak{I}_{h,\partial}^q p$ into $\text{span } \Psi_{h,\circ}^q|_K$, it is $\mathfrak{I}_{h,\circ}^q p = p - \mathfrak{I}_{h,\partial}^q p$ and the second statement of the lemma follows. \square

A consequence of this lemma is that

$$\mathcal{P}^q(K) \subset \text{span } \Psi_h^q|_K,$$

i.e. the space of polynomials of degree q is locally embedded in the approximation space over each element. Obviously, the element basis functions are essential to capture the non-harmonic polynomials.

Lemma 3. *The restrictions of the interpolation operators $\mathfrak{I}_{h,\partial}^q$ and \mathfrak{I}_h^q onto an element $K \in \mathcal{K}_h$ of a regular and stable mesh \mathcal{K}_h with $h_K = 1$ are linear and continuous. Furthermore, there are constants c each, which solely depend on the regularity and stability parameters of the mesh, such that*

$$\|\mathfrak{I}_{h,\partial}^q v\|_{H^1(K)} \leq c \|v\|_{H^2(K)} \quad \text{and} \quad \|\mathfrak{I}_h^q v\|_{H^1(K)} \leq c \|v\|_{H^2(K)}$$

for all $v \in H^2(K)$.

Proof. The linearity of the operators is obvious, so we only have to prove the given estimates which also ensure the continuity.

First, we construct an auxiliary triangulation $\mathcal{T}_h(K)$ of K by connecting the nodes on the boundary of K with the point z_K from Definition 1, see Figure 3. This triangular mesh is regular in the classical sense, i.e. neighbouring triangles share either a common node or edge and the aspect ratio of each triangle is uniformly bounded by some constant $\sigma_{\mathcal{T}}$. The boundedness of the aspect ratio can be seen

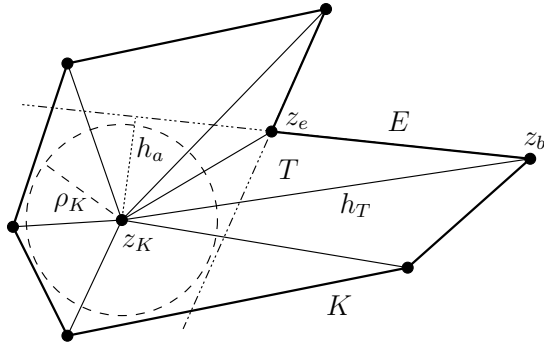


Figure 3: Auxiliary triangulation $\mathcal{T}_h(K)$ of star-shaped element K , and altitude h_a of the triangle T perpendicular to E

as follows. Let $T \in \mathcal{T}_h(K)$ be a triangle with diameter h_T and let ρ_T be the radius of the incircle. It is known that the area of T is given as $A_T = \frac{1}{2}U_T\rho_T$, where U_T is the perimeter of T . The perimeter can be bounded from above by $U_T \leq 3h_T$. On the other hand, we have the formula $A_T = \frac{1}{2}h_E h_a$, where h_a is the altitude of the triangle perpendicular to E , see Figure 3. Since the element K is star-shaped with respect to a circle of radius ρ_K , the line through the side $E \in \mathcal{E}_h$ of the triangle does not intersect this circle. Thus, it is $h_a \geq \rho_K$ and we have the estimate $A_T \geq \frac{1}{2}h_E\rho_K$. Together with the Definitions 1 and 2, we obtain

$$\frac{h_T}{\rho_T} = \frac{U_T h_T}{2A_T} \leq \frac{3h_T^2}{h_E \rho_K} \leq \frac{3h_T^2}{(h_K/c_K)(h_K/\sigma_K)} \leq 3c_K \sigma_K = \sigma_{\mathcal{T}}.$$

On this auxiliary triangulation, we can use classical interpolation operators, see e.g. [8]. Let

$$\mathfrak{I}_{\mathcal{T}} : H^2(K) \rightarrow \mathcal{P}_{\text{pw}}^q(\mathcal{T}_h(K))$$

be such a classical operator with

$$\|v - \mathfrak{I}_{\mathcal{T}}v\|_{H^1(K)} \leq C_{\mathcal{T}} h_{\mathcal{T}} |v|_{H^2(K)} \quad \text{for } v \in H^2(K), \quad (12)$$

where $h_{\mathcal{T}} = \max\{h_T : T \in \mathcal{T}_h(K)\}$ and

$$\mathcal{P}_{\text{pw}}^q(\mathcal{T}_h(K)) = \{p \in C^0(K) : p|_T \in \mathcal{P}^q(T) \quad \forall T \in \mathcal{T}_h(K)\}.$$

The constant $C_{\mathcal{T}}$ solely depends on $\sigma_{\mathcal{T}}$ and thus on the regularity and stability parameters of the polygonal mesh \mathcal{K}_h .

Next, we prove the continuity of $\mathfrak{I}_{h,\partial}^q$, i.e. the estimate

$$\|\mathfrak{I}_{h,\partial}^q v\|_{H^1(K)} \leq c \|v\|_{H^2(K)} \quad \text{for } v \in H^2(K).$$

Let $v \in H^2(K)$ be fixed. The interpolation $\mathfrak{I}_{h,\partial}^q v$ fulfills the boundary value problem

$$\begin{aligned} -\Delta u &= 0 & \text{in } K, \\ u &= g_v & \text{on } \partial K, \end{aligned}$$

where $g_v = \mathfrak{J}_{h,\partial}^q v|_{\partial K}$ is a piecewise polynomial of degree q on ∂K . We write $u = u_0 + u_g$ with $u_g = \mathfrak{J}_{\mathcal{T}} v$ and obtain the Galerkin formulation

$$\text{Find } u_0 \in H_0^1(K) : \quad (\nabla u_0, \nabla w)_{L_2(K)} = -(\nabla u_g, \nabla w)_{L_2(K)} \quad \text{for } w \in H_0^1(K)$$

which has a unique solution. Testing with $w = u_0$ and applying the Cauchy–Schwarz inequality yield

$$|u_0|_{H^1(K)}^2 \leq |(\nabla u_g, \nabla u_0)_{L_2(K)}| \leq |u_g|_{H^1(K)} |u_0|_{H^1(K)},$$

and consequently

$$|u_0|_{H^1(K)} \leq \|u_g\|_{H^1(K)} = \|\mathfrak{J}_{\mathcal{T}} v\|_{H^1(K)}.$$

The lower triangular inequality applied to (12) gives

$$\|\mathfrak{J}_{\mathcal{T}} v\|_{H^1(K)} - \|v\|_{H^1(K)} \leq \|v - \mathfrak{J}_{\mathcal{T}} v\|_{H^1(K)} \leq C_{\mathcal{T}} h_{\mathcal{T}} |v|_{H^2(K)}$$

and, since $h_{\mathcal{T}} \leq h_K = 1$, we obtain by rearranging

$$\|\mathfrak{J}_{\mathcal{T}} v\|_{H^1(K)} \leq c \|v\|_{H^2(K)}.$$

Because of the piecewise smoothness of the boundary of K and since it can be embedded into a square of side length h_K , the Poincaré–Friedrichs inequality can be written as

$$\|w\|_{L_2(K)} \leq h_K |w|_{H^1(K)} \quad \text{for } w \in H_0^1(K),$$

see e.g. [6]. By the use of the given estimates and $h_K = 1$, we obtain

$$\begin{aligned} \|\mathfrak{J}_{h,\partial}^q v\|_{H^1(K)} &\leq \|u_0\|_{H^1(K)} + \|u_g\|_{H^1(K)} \\ &= \left(\|u_0\|_{L_2(K)}^2 + |u_0|_{H^1(K)}^2 \right)^{1/2} + \|\mathfrak{J}_{\mathcal{T}} v\|_{H^1(K)} \\ &\leq \sqrt{2} |u_0|_{H^1(K)} + \|\mathfrak{J}_{\mathcal{T}} v\|_{H^1(K)} \\ &\leq (\sqrt{2} + 1) \|\mathfrak{J}_{\mathcal{T}} v\|_{H^1(K)} \\ &\leq c \|v\|_{H^2(K)}. \end{aligned}$$

Finally, we use the continuity of $\mathfrak{J}_{h,\partial}^q$ as well as the property (10) of $\mathfrak{J}_{h,\circ}^q$ with $h_K = 1$ and we get

$$\begin{aligned} \|\mathfrak{J}_h^q v\|_{H^1(K)} &\leq \|\mathfrak{J}_{h,\partial}^q v\|_{H^1(K)} + \|\mathfrak{J}_{h,\circ}^q v\|_{H^1(K)} \\ &\leq \|\mathfrak{J}_{h,\partial}^q v\|_{H^1(K)} + \|v - \mathfrak{J}_{h,\partial}^q v\|_{H^1(K)} \\ &\leq \|v\|_{H^1(K)} + 2\|\mathfrak{J}_{h,\partial}^q v\|_{H^1(K)} \\ &\leq c \|v\|_{H^2(K)} \end{aligned}$$

that concludes the proof. \square

Remark 2. The stability of the mesh \mathcal{K}_h was only needed to prove the uniform boundedness of the aspect ratios in the auxiliary triangulations of the star-shaped elements. If we go without the stability but ensure convexity of the elements we can prove a maximum angle condition for the auxiliary triangulations, see [28]. In this case, the classical interpolation operator from [18] can be used to prove the continuity of \mathfrak{I}_h^q . Consequently, the lemma stays valid for convex elements even if the edge length h_E decreases faster than the element diameter h_K and violates the uniform estimate $h_K \leq c_{\mathcal{K}} h_E$.

Definition 3. A mesh or a family of meshes is called admissible if it is either regular and stable or it is only regular but with solely convex elements. The mesh parameters are $(\sigma_{\mathcal{K}}, c_{\mathcal{K}})$ and $\sigma_{\mathcal{K}}$, respectively.

The condition $h_K = 1$ in Lemma 3 is not fulfilled in general. Thus, we introduce a scaling for the elements $K \in \mathcal{K}_h$ such that

$$\widehat{K} \ni \widehat{x} \mapsto x = F_K(\widehat{x}) = h_K \widehat{x} \in K. \quad (13)$$

Consequently, it is $h_{\widehat{K}} = 1$ and we set $\widehat{v} = v \circ F_K$. Simple calculations show that for $v \in H^k(K)$, $k \in \mathbb{N}_0$ it is $\widehat{v} \in H^k(\widehat{K})$ and

$$|\widehat{v}|_{H^k(\widehat{K})} = h_K^{k-1} |v|_{H^k(K)}. \quad (14)$$

Additionally, it is

$$(u, v)_{L_2(K)} = h_K^2 (\widehat{u}, \widehat{v})_{L_2(\widehat{K})} \quad \text{and} \quad (\nabla u, \nabla v)_{L_2(K)} = (\widehat{\nabla} \widehat{u}, \widehat{\nabla} \widehat{v})_{L_2(\widehat{K})}$$

for $u, v \in H^1(K)$, where $\widehat{\nabla}$ denotes the gradient with respect to \widehat{x} . According to the definition of the weighted scalar product, see (8), we obtain

$$(u, v)_{hH^1(K)} = h_K^2 (\widehat{u}, \widehat{v})_{hH^1(\widehat{K})}. \quad (15)$$

Lemma 4. *The restrictions of the interpolation operators $\mathfrak{I}_{h,\partial}^q$ and \mathfrak{I}_h^q onto an element $K \in \mathcal{K}_h$ fulfill for $v \in H^2(K)$*

$$\widehat{\mathfrak{I}_{h,\partial}^q v} = \widehat{\mathfrak{I}_{h,\partial}^q} \widehat{v} \quad \text{and} \quad \widehat{\mathfrak{I}_h^q v} = \widehat{\mathfrak{I}_h^q} \widehat{v},$$

where $\widehat{\mathfrak{I}_h^q} = \widehat{\mathfrak{I}_{h,\circ}^q} + \widehat{\mathfrak{I}_{h,\partial}^q}$ and $\widehat{\mathfrak{I}_{h,\partial}^q}$ as well as $\widehat{\mathfrak{I}_{h,\circ}^q}$ are the interpolation operators with respect to the scaled element \widehat{K} .

Proof. Due to the pointwise definition of $\mathfrak{I}_{h,\partial}^q$ and the construction of the nodal and edge basis functions, it is obvious that $\widehat{\mathfrak{I}_{h,\partial}^q v} = \widehat{\mathfrak{I}_{h,\partial}^q} \widehat{v}$. Therefore, we only have to show $\widehat{\mathfrak{I}_{h,\circ}^q v} = \widehat{\mathfrak{I}_{h,\circ}^q} \widehat{v}$ with $\widehat{\mathfrak{I}_{h,\circ}^q} : H^2(\widehat{K}) \rightarrow \text{span} \{\psi_{\widehat{K},i,j}\}$. Furthermore, it is sufficient to prove

$$\widehat{\mathfrak{I}_{h,\circ}^q v} \in \text{span} \{\psi_{\widehat{K},i,j}\}$$

and

$$(\widehat{\mathfrak{J}_{h,\circ}^q v}, \varphi)_{H^1(\widehat{K})} = (\widehat{\mathfrak{J}_{h,\circ}^q \widehat{v}}, \varphi)_{H^1(\widehat{K})} \quad \forall \varphi \in \text{span} \{\psi_{\widehat{K},i,j}\},$$

since for $\varphi = \widehat{\mathfrak{J}_{h,\circ}^q v} - \widehat{\mathfrak{J}_{h,\circ}^q \widehat{v}}$, we obtain

$$\|\widehat{\mathfrak{J}_{h,\circ}^q v} - \widehat{\mathfrak{J}_{h,\circ}^q \widehat{v}}\|_{H^1(\widehat{K})} = 0 \quad \text{and thus} \quad \widehat{\mathfrak{J}_{h,\circ}^q v} = \widehat{\mathfrak{J}_{h,\circ}^q \widehat{v}}.$$

Here, we have skipped the ranges of i, j for shorter notation. In the definition of the element basis functions $\psi_{K,i,j}$, see (3), we have made no specific choice of the polynomials $p_{K,i,j}$. In the following, let the polynomials for the functions $\psi_{\widehat{K},i,j}$ over \widehat{K} be chosen in dependence of $\psi_{K,i,j}$ as

$$p_{\widehat{K},i,j} = h_K^2 \widehat{p}_{K,i,j}.$$

In consequence, we obtain for the scaled element function $\widehat{\psi}_{K,i,j} = \psi_{K,i,j} \circ F_K$ that

$$-\widehat{\Delta} \widehat{\psi}_{K,i,j} = h_K^2 \widehat{p}_{K,i,j} = p_{\widehat{K},i,j} = -\widehat{\Delta} \psi_{\widehat{K},i,j} \quad \text{in } \widehat{K}$$

and $\widehat{\psi}_{K,i,j} = \psi_{\widehat{K},i,j}$ on ∂K , where $\widehat{\Delta}$ denotes the Laplace operator with respect to \widehat{x} . Due to the unique solvability of the Dirichlet problem for the Laplace equation, we get $\psi_{\widehat{K},i,j} = \widehat{\psi}_{K,i,j}$ and thus

$$\widehat{\mathfrak{J}_{h,\circ}^q v} = \sum_{i=0}^{q-2} \sum_{j=0}^i v_{K,i,j} \widehat{\psi}_{K,i,j} \in \text{span} \{\psi_{\widehat{K},i,j}\}.$$

Next, let $\varphi_{\widehat{K}} \in \text{span} \{\psi_{\widehat{K},i,j}\}$ and set $\varphi_K = \varphi_{\widehat{K}} \circ F_K^{-1} \in \text{span} \{\psi_{K,i,j}\}$. By the definition of $\mathfrak{J}_{h,\circ}^q$, it is

$$(\mathfrak{J}_{h,\circ}^q v, \varphi_K)_{hH^1(K)} = (v - \mathfrak{J}_{h,\partial}^q v, \varphi_K)_{hH^1(K)}.$$

Applying (15) to both sides of the equation yields

$$\begin{aligned} (\widehat{\mathfrak{J}_{h,\circ}^q v}, \varphi_{\widehat{K}})_{H^1(\widehat{K})} &= (v - \widehat{\mathfrak{J}_{h,\partial}^q v}, \varphi_{\widehat{K}})_{H^1(\widehat{K})} \\ &= (\widehat{v} - \widehat{\mathfrak{J}_{h,\partial}^q \widehat{v}}, \varphi_{\widehat{K}})_{H^1(\widehat{K})} \\ &= (\widehat{\mathfrak{J}_{h,\circ}^q \widehat{v}}, \varphi_{\widehat{K}})_{H^1(\widehat{K})}, \end{aligned}$$

where the last equality comes from the definition of $\widehat{\mathfrak{J}_{h,\circ}^q}$ and the fact that the scalar products $(\cdot, \cdot)_{hH^1(\widehat{K})}$ and $(\cdot, \cdot)_{H^1(\widehat{K})}$ coincide on the scaled element. Since $\varphi_{\widehat{K}}$ is chosen arbitrarily, this equality concludes the proof. \square

Theorem 1. For an admissible mesh \mathcal{K}_h of a bounded polygonal domain $\Omega \subset \mathbb{R}^2$, the interpolation operators $\mathfrak{I}_{h,\partial}^q$ and \mathfrak{I}_h^q fulfill

$$\|v - \mathfrak{I}_{h,\partial}^q v\|_{H^\ell(\Omega)} \leq c h^{q+1-\ell} |v|_{H^{q+1}(\Omega)} \quad \text{for } v \in H_{\Delta}^{q+1}(\mathcal{K}_h),$$

and

$$\|v - \mathfrak{I}_h^q v\|_{H^\ell(\Omega)} \leq c h^{q+1-\ell} |v|_{H^{q+1}(\Omega)} \quad \text{for } v \in H^{q+1}(\Omega),$$

respectively, where $h = \max\{h_K : K \in \mathcal{K}_h\}$, $\ell = 0, 1$ and the constant c solely depends on the mesh parameters.

Proof. First, we consider the second estimate and the case $\ell = 1$. Let us start to examine the error over one element $K \in \mathcal{K}_h$. We scale this element in such a way that its diameter becomes one, see (13). With the help of (14) and Lemma 4, we obtain

$$\begin{aligned} \|v - \mathfrak{I}_h^q v\|_{H^1(K)}^2 &= \|v - \mathfrak{I}_h^q v\|_{L_2(K)}^2 + |v - \mathfrak{I}_h^q v|_{H^1(K)}^2 \\ &\leq c h_K^2 \|\widehat{v} - \widehat{\mathfrak{I}}^q \widehat{v}\|_{L_2(\widehat{K})}^2 + c |\widehat{v} - \widehat{\mathfrak{I}}^q \widehat{v}|_{H^1(\widehat{K})}^2 \\ &\leq c \|\widehat{v} - \widehat{\mathfrak{I}}^q \widehat{v}\|_{H^1(\widehat{K})}^2 \end{aligned}$$

since $h_K \leq 1$. Let $\widehat{p} \in \mathcal{P}^q(\widehat{K})$ be the polynomial of the Bramble–Hilbert Lemma for star-shaped domains, which closely approximates \widehat{v} , see [7]. It fulfills

$$\|\widehat{v} - \widehat{p}\|_{H^k(\widehat{K})} \leq C h_{\widehat{K}}^{q+1-k} |\widehat{v}|_{H^{q+1}(\widehat{K})} \quad \text{for } k = 0, 1, \dots, q+1 \quad (16)$$

with a constant C that only depends on $\sigma_{\mathcal{K}}$ and q . Due to the scaling $h_{\widehat{K}} = 1$ and by the application of Lemmata 2 and 3, we obtain

$$\begin{aligned} \|\widehat{v} - \widehat{\mathfrak{I}}^q \widehat{v}\|_{H^1(\widehat{K})} &\leq \|\widehat{v} - \widehat{p}\|_{H^1(\widehat{K})} + \|\widehat{\mathfrak{I}}^q(\widehat{v} - \widehat{p})\|_{H^1(\widehat{K})} \\ &\leq (1+c) \|\widehat{v} - \widehat{p}\|_{H^2(\widehat{K})} \\ &\leq (1+c)C |\widehat{v}|_{H^{q+1}(\widehat{K})}, \end{aligned} \quad (17)$$

where we have used (16) in the last step. Comparing the previous estimates and transforming back to the element K yields

$$\|v - \mathfrak{I}_h^q v\|_{H^1(K)}^2 \leq c h_K^{2q} |v|_{H^{q+1}(K)}^2.$$

Finally, we have to sum up this inequality over all elements of the mesh and apply the square root to it. This gives

$$\|v - \mathfrak{I}_h^q v\|_{H^1(\Omega)} \leq c \left(\sum_{K \in \mathcal{K}_h} h_K^{2q} |v|_{H^{q+1}(K)}^2 \right)^{1/2} \leq c h^q |v|_{H^{q+1}(\Omega)},$$

and finishes the proof for $\ell = 1$. The case $\ell = 0$ follows by

$$\|v - \mathfrak{I}_h^q v\|_{L_2(K)} = h_K \|\widehat{v} - \widehat{\mathfrak{I}}_h^q \widehat{v}\|_{L_2(\widehat{K})} \leq h_K \|\widehat{v} - \widehat{\mathfrak{I}}_h^q \widehat{v}\|_{H^1(\widehat{K})}$$

and the same arguments as above.

The error estimate for $\mathfrak{I}_{h,\partial}^q$ follows in the same way. The case $q = 1$ is already proven since $\mathfrak{I}_{h,\partial}^1 = \mathfrak{I}_h^1$, thus let $q \geq 2$. The only point, where we have to take special care, is in (16). We have to ensure that \widehat{p} is harmonic. In the formulation of the Bramble–Hilbert Lemma in [7], \widehat{p} is chosen as Taylor polynomial of \widehat{v} averaged over the circle given in Definition 1. Furthermore, the commutativity is proven for the operator of the weak derivative and the operator for the averaged Taylor polynomial for $q \geq 2$. Thus, since $\widehat{v} \in H^2(\widehat{K})$ and $\widehat{\Delta}\widehat{v} = 0$ in the weak sense, we obtain that the averaged Taylor polynomial \widehat{p} is harmonic. \square

4 BEM-based Finite Element Method

In the previous section we have discussed the discretization of the Sobolev space $H^1(\Omega)$ and investigated approximation properties. Thus, we come back to the model problem (1) and formulate the BEM-based Finite Element Method with the use of the introduced arbitrary order basis functions.

4.1 Galerkin formulation and convergence estimates

For inhomogeneous Dirichlet data g_D , we extend it into the interior of the domain. The extension is denoted by g_D again, and we assume that it can be chosen such that $g_D \in V_h^q$. Let

$$V_{h,D}^q = V_h^q \cap H_D^1(\Omega) \quad \text{with} \quad H_D^1(\Omega) = \{v \in H^1(\Omega) : v|_{\Gamma_D} = 0\}.$$

The discrete Galerkin formulation for the model problem (1) reads:

$$\text{Find } u_h \in g_D + V_{h,D}^q : b(u_h, v_h) = (f, v_h)_{L_2(\Omega)} + (g_N, v_h)_{L_2(\Gamma_N)} \quad \forall v_h \in V_{h,D}^q, \quad (18)$$

where

$$b(\psi, \varphi) = (a \nabla \psi, \nabla \varphi)_{L_2(\Omega)}$$

is the well known bilinear form for the diffusion problem. Due to the boundedness of the diffusion coefficient, the bilinear form $b(\cdot, \cdot)$ is bounded and coercive on $H_D^1(\Omega)$. Because of the conforming approximation space $V_D^q \subset H_D^1(\Omega)$, the Galerkin formulation above admits a unique solution according to the Lax–Milgram Lemma. Céa’s Lemma yields

$$\|u - u_h\|_{H^1(\Omega)} \leq c \min_{v_h \in g_D + V_{h,D}^q} \|u - v_h\|_{H^1(\Omega)}.$$

This quasi best approximation gives rise to error estimates for the finite element formulation. The minimum on the right hand side can be estimated from above by setting $v_h = \mathfrak{I}_h^q u$. By the use of the interpolation properties given in Theorem 1, we obtain the next result.

Theorem 2. *Let \mathcal{K}_h be an admissible mesh of the bounded polygonal domain $\Omega \subset \mathbb{R}^2$. Then, the solution $u_h \in V_h^q$ of the Galerkin formulation from above fulfills*

$$\|u - u_h\|_{H^1(\Omega)} \leq c h^q |u|_{H^{q+1}(\Omega)} \quad \text{for } u \in H^{q+1}(\Omega),$$

where $h = \max\{h_K : K \in \mathcal{K}_h\}$ and the constant c solely depends on the mesh parameters.

If we assume more regularity for the model problem, the Aubin–Nitsche trick together with Theorem 2 can be used to prove an error estimate in the L^2 -norm, see, e.g., [7].

Theorem 3. *Let \mathcal{K}_h be an admissible mesh of the bounded polygonal domain $\Omega \subset \mathbb{R}^2$ and let there be, for any $g \in L_2(\Omega)$, a unique solution of*

$$\text{Find } w \in H_D^1(\Omega) : \quad b(v, w) = (g, v)_{L_2(\Omega)} \quad \forall v \in H_D^1(\Omega),$$

with $w \in H^2(\Omega)$ such that

$$|w|_{H^2(\Omega)} \leq C \|g\|_{L_2(\Omega)}.$$

Then, the solution $u_h \in V_h^q$ of the Galerkin formulation from above fulfills

$$\|u - u_h\|_{L_2(\Omega)} \leq c h^{q+1} |u|_{H^{q+1}(\Omega)} \quad \text{for } u \in H^{q+1}(\Omega),$$

where the constant c solely depends on the mesh parameters.

If the boundary value problem (1) has homogeneous right hand side, i.e. $f = 0$, and thus the solution fulfills $u \in H_\Delta^1(\mathcal{K}_h)$, we can seek the approximation u_h directly in the subspace $V_{h,\partial}^q = \text{span } \Psi_{h,\partial}^q \subset V_h^q$. Consequently, we obtain a reduced Galerkin formulation. The same arguments as above yield optimal rates of convergence, when the interpolation operator $\mathfrak{I}_{h,\partial}^q$ is used instead of \mathfrak{I}_h^q .

Theorem 4. *Under the same assumptions as in Theorems 2 and 3, the solution $u_h \in V_{h,\partial}^q$ of the reduced Galerkin formulation fulfills*

$$\|u - u_h\|_{H^\ell(\Omega)} \leq c h^{q+1-\ell} |u|_{H^{q+1}(\Omega)} \quad \text{for } u \in H_\Delta^{q+1}(\mathcal{K}_h),$$

where $\ell = 0, 1$ and the constant c solely depends on the mesh parameters.

In the implementation, however, the bilinear form $b(\cdot, \cdot)$ cannot be evaluated analytically since the basis function are only given implicitly as solutions of local boundary value problems. Thus, we make use of local boundary integral formulations which are approximated by the help of Boundary Element Methods.

4.2 Boundary Element Method

The ansatz functions locally fulfill Dirichlet problems for the Laplace and Poisson equation. Without loss of generality, we just focus on the Laplace equation. In the case of element basis functions, which fulfill the Poisson equation, see (3), we reformulate their definition. For this purpose, we decompose $\psi_K = \psi_K^0 + \psi_K^p \in \Psi_{h,\circ}^q$, where $\psi_K^p \in \mathcal{P}^q(K)$ is a particular solution of $-\Delta\psi_K^p = p_K$. The polynomial ψ_K^p can be constructed for any right hand side $p_K \in \mathcal{P}^{q-2}(K)$ according to [20]. Thus, for fixed ψ_K^p , we end up with a Laplace problem for ψ_K^0 . So, let us consider

$$\begin{aligned} -\Delta\psi &= 0 \quad \text{in } K, \\ \psi &= g \quad \text{on } \partial K, \end{aligned} \tag{19}$$

for an arbitrary element $K \in \mathcal{K}_h$ and some piecewise polynomial function g on ∂K . In the following, the usual trace operator $\gamma_0^K : H^1(K) \rightarrow H^{1/2}(\partial K)$ is needed which is defined in [1], for example. Let $v \in H^1(K)$ with Δv in the dual of $H^1(K)$. Due to Green's first identity [22], there exists a unique function $\gamma_1^K v \in H^{-1/2}(\partial K)$ such that

$$\int_K \nabla v(y) \cdot \nabla w(y) dy = \int_{\partial K} \gamma_1^K v(y) \gamma_0^K w(y) ds_y - \int_K w(y) \Delta v(y) dy \tag{20}$$

for $w \in H^1(K)$. We call $\gamma_1^K v$ the conormal derivative of v . If v is sufficiently smooth, like $v \in H^2(K)$, we have

$$(\gamma_1^K v)(x) = n_K(x) \cdot (\gamma_0^K \nabla v)(x) \quad \text{for } x \in \partial K,$$

where $n_K(x)$ denotes the outer normal vector of the element K at x . Therefore, the conormal derivative is also called Neumann trace for the Laplace equation. Both operators, the Dirichlet trace γ_0^K and the Neumann trace γ_1^K , are linear and continuous. By the use of these traces, the solution of (19) can be written as

$$\psi(x) = \int_{\partial K} U^*(x, y) \gamma_1^K \psi(y) ds_y - \int_{\partial K} \gamma_{1,y}^K U^*(x, y) \gamma_0^K \psi(y) ds_y \quad \text{for } x \in K, \tag{21}$$

where U^* is the fundamental solution of minus the Laplacian with

$$U^*(x, y) = -\frac{1}{2\pi} \ln|x - y| \quad \text{for } x, y \in \mathbb{R}^2,$$

see, e.g., [22]. Equation (21) is the so called representation formula. The Dirichlet trace $\gamma_0^K \psi = g$ is known by the problem (19) and the Neumann trace $\gamma_1^K \psi$ is an unknown quantity. However, as soon as we have an expression for the Neumann trace, the representation formula can be used to evaluate the solution of (19) everywhere inside of K .

Applying the trace operators to (21) yields, after some calculations, the relationship

$$\gamma_1^K \psi = \mathbf{S}_K \gamma_0^K \psi \quad \text{with} \quad \mathbf{S}_K = \mathbf{V}_K^{-1} \left(\frac{1}{2} \mathbf{I} + \mathbf{K}_K \right), \quad (22)$$

see [22, 29]. The operator $\mathbf{S}_K : H^{1/2}(\partial K) \rightarrow H^{-1/2}(\partial K)$ is called Steklov-Poincaré operator. For $x \in \partial K$, we have the single-layer potential operator

$$(\mathbf{V}_K \vartheta)(x) = \gamma_0^K \int_{\partial K} U^*(x, y) \vartheta(y) ds_y \quad \text{for } \vartheta \in H^{-1/2}(\partial K),$$

as well as the double-layer potential operator

$$(\mathbf{K}_K \xi)(x) = \lim_{\varepsilon \rightarrow 0} \int_{y \in \partial K: |y-x| \geq \varepsilon} \gamma_{1,y}^K U^*(x, y) \xi(y) ds_y \quad \text{for } \xi \in H^{1/2}(\partial K).$$

Due to the assumption $h_K < 1$, the single-layer potential operator is invertible. Further computations give the symmetric representation of the Steklov-Poincaré operator

$$\mathbf{S}_K = \mathbf{D}_K + \left(\frac{1}{2} \mathbf{I} + \mathbf{K}'_K \right) \mathbf{V}_K^{-1} \left(\frac{1}{2} \mathbf{I} + \mathbf{K}_K \right)$$

which involves the adjoint double layer potential \mathbf{K}'_K as well as the hypersingular integral operator

$$\mathbf{D}_K \xi = -\gamma_1^K \int_{\partial K} \gamma_{1,y}^K U^*(\cdot, y) \xi(y) ds_y \quad \text{for } \xi \in H^{1/2}(\partial K).$$

For more details on these classical boundary integral operators, we refer the reader to [22, 29].

To obtain an approximation of the Neumann trace, we utilize a Boundary Element Method. So, we apply the Galerkin scheme over the boundary of the element. The Dirichlet data of (19) is given as

$$g \in \mathcal{P}_{\text{pw}}^q(\partial K) = \{p \in C^0(\partial K) : p|_E \in \mathcal{P}^q(E) \quad \forall E \in \mathcal{E}(K)\} \subset H^{1/2}(\partial K),$$

where $\mathcal{E}(K)$ denotes the set of all edges which lie inside the boundary of K . Furthermore, it is easy to see that

$$\Phi^q(\partial K) = \{\gamma_0^K \varphi : \varphi \in \Psi_{h,\partial}^q|_K\}$$

is a basis of $\mathcal{P}_{\text{pw}}^q(\partial K)$. The Neumann trace $\gamma_1^K \psi$ is approximated in the space

$$\mathcal{P}_{\text{pw,d}}^{q-1}(\partial K) = \{p \in L_2(\partial K) : p|_E \in \mathcal{P}^{q-1}(E) \quad \forall E \in \mathcal{E}(K)\} \subset H^{-1/2}(\partial K)$$

with some basis $\Phi_d^{q-1}(\partial K)$. The discrete variational formulation of (22) to find an approximation t of $\gamma_1^K \psi$ reads

$$\text{Find } t \in \mathcal{P}_{\text{pw,d}}^{q-1}(\partial K) : (\mathbf{V}_K t, \vartheta)_{L_2(\partial K)} = \left(\left(\frac{1}{2} \mathbf{I} + \mathbf{K}_K \right) g, \vartheta \right)_{L_2(\partial K)} \quad \forall \vartheta \in \Phi_d^{q-1}(\partial K).$$

This problem admits a unique solution due to the properties of the boundary integral operators. Expressing g and t as linear combinations of the basis functions taken from $\Phi^q(\partial K)$ and $\Phi_d^{q-1}(\partial K)$, respectively, and denoting the coefficient vectors by \underline{g} and \underline{t} gives the matrix form

$$\underline{\mathbf{V}}_K \underline{t} = \left(\frac{1}{2} \underline{\mathbf{M}}_K + \underline{\mathbf{K}}_K \right) \underline{g}$$

of the discrete variational formulation. Here, $\underline{\mathbf{M}}_K$ is the mass matrix and the other matrices correspond to the boundary integral operators applied to ansatz functions and tested with ansatz functions. For a more detailed description see [28] or any boundary element literature, e.g. [29]. As soon as this system of linear equations is solved, the exact Neumann trace $\gamma_1^K \psi$ in (21) can be replaced by t to get an approximation of ψ inside of K . Additionally, we define the approximation

$$\tilde{\mathbf{S}}_K g = \mathbf{D}_K g + \left(\frac{1}{2} \mathbf{I} + \mathbf{K}'_K \right) t$$

of the symmetric representation of the Steklov-Poincaré operator. By the use of $\tilde{\mathbf{S}}_K$, we introduce the symmetric matrix

$$\underline{\mathbf{S}}_K = \left(\left(\tilde{\mathbf{S}}_K \xi, \zeta \right)_{L_2(\partial K)} \right)_{\xi, \zeta \in \Phi_D}$$

which has the form

$$\underline{\mathbf{S}}_K = \underline{\mathbf{D}}_K + \left(\frac{1}{2} \underline{\mathbf{M}}_K^\top + \underline{\mathbf{K}}_K^\top \right) \underline{\mathbf{V}}_K^{-1} \left(\frac{1}{2} \underline{\mathbf{M}}_K + \underline{\mathbf{K}}_K \right).$$

These boundary element matrices are dense and their entries involve singular integrals. However, they are well studied and efficient algorithms exist for their set up and their storage, see [26]. The main computational effort is the inversion of the single-layer potential matrix which is realized by the use of an efficient LAPACK routine in our numerical experiments. For the BEM-based FEM these matrices are utilized for each element and matrices to different elements are independent. Thus, they are set up in parallel once in a preprocessing step. Furthermore, the Boundary Element Method is directly applied on the naturally given polygonal boundary of the elements without further discretization. Consequently, the resulting boundary element matrices are rather small and the local complexity is negligible compared to the complexity of the global problem.

4.3 Approximation of the Galerkin formulation

In the realization of the discrete Galerkin formulation (18), we have to address the evaluation of the bilinear form applied to ansatz functions. Since the diffusion

coefficient is assumed to be constant on each element such that $a(\cdot) = a_K \in \mathbb{R}$ on K , for $K \in \mathcal{K}_h$, we have

$$b(\psi, \varphi) = (a\nabla\psi, \nabla\varphi)_{L_2(\Omega)} = \sum_{K \in \mathcal{K}_h} a_K (\nabla\psi, \nabla\varphi)_{L_2(K)} \quad \text{for } \psi, \varphi \in \Psi_h^q.$$

We remember that the basis $\Psi_h^q = \Psi_{h,\partial}^q \cup \Psi_{h,\circ}^q$ consists of piecewise harmonic functions and element bubble functions which vanish on the element boundaries. According to (6), it holds

$$b(\psi, \varphi) = 0 \quad \text{for } \psi \in \Psi_{h,\partial}^q, \varphi \in \Psi_{h,\circ}^q, \quad (23)$$

and thus the discrete Galerkin formulation (18) decouples. If we split the unknown function into

$$u_h = u_{h,\partial} + u_{h,\circ} \quad \text{with } u_{h,\partial} \in V_{h,\partial}^q \quad \text{and } u_{h,\circ} \in V_{h,\circ}^q,$$

and take $g_D \in V_{h,\partial}^q$, we obtain with $V_{h,\partial,D}^q = V_{h,\partial}^q \cap H_D^1(\Omega)$

$$\begin{aligned} \text{Find } u_{h,\partial} \in g_D + V_{h,\partial,D}^q : \\ b(u_{h,\partial}, v_h) = (f, v_h)_{L_2(\Omega)} + (g_N, v_h)_{L_2(\Gamma_N)} \quad \forall v_h \in V_{h,\partial,D}^q, \end{aligned} \quad (24)$$

and

$$\text{Find } u_{h,\circ} \in V_{h,\circ}^q : \quad b(u_{h,\circ}, v_h) = (f, v_h)_{L_2(\Omega)} \quad \forall v_h \in V_{h,\circ}^q. \quad (25)$$

A closer look at (25) shows that $u_{h,\circ}|_K \in H_0^1(K)$, $K \in \mathcal{K}_h$ is the orthogonal projection of f/a_K into $\text{span } \Psi_{h,\circ}^q|_K$ with respect to the scalar product $(\nabla \cdot, \nabla \cdot)_{L_2(K)}$. Thus, $u_{h,\circ}$ is separated from the global problem and can be computed via local projections. The problem (24) turns into a global system of linear equations with a symmetric and positive definite matrix.

It remains to discuss the approximations of the terms

$$b(\psi, \varphi), \quad (f, \varphi)_{L_2(\Omega)} \quad \text{and} \quad (g_N, \varphi)_{L_2(\Gamma_N)} \quad \text{for } \psi, \varphi \in \Psi_h^q.$$

The last term is rather simple. The Neumann data g_N is given and the ansatz functions φ are piecewise polynomial of order q on the Neumann boundary Γ_N . Thus, we split the L_2 -scalar product over Γ_N into its contributions over each edge in the boundary and use standard Gaussian quadrature.

To handle the L_2 -scalar product over Ω , we use a quadrature over polygonal elements. This can be done by refining the elements into triangles or by using a numerical integration scheme for polygonal domains, see [23]. The evaluations of the ansatz functions in the quadrature points are realized with the help of the representation formula (21).

So, we come to the bilinear form. If $\psi, \varphi \in \Psi_{h,\partial}^q$, Green's first identity (20) is used on each element. This yields

$$b(\psi, \varphi) = \sum_{K \in \mathcal{K}_h} a_K \int_{\partial K} \gamma_1^K \psi \gamma_0^K \varphi,$$

where the volume integrals have vanished since the ansatz functions fulfill the Laplace equation on each element. Thus, we are able to reduce the evaluation of the bilinear form to integration over element boundaries. According to Subsection 4.2, we have

$$\int_{\partial K} \gamma_1^K \psi \gamma_0^K \varphi = \int_{\partial K} \gamma_0^K \varphi \mathbf{S}_K \gamma_0^K \psi \approx \int_{\partial K} \gamma_0^K \varphi \tilde{\mathbf{S}}_K \gamma_0^K \psi = (\underline{\gamma_0^K \varphi})^\top \underline{\mathbf{S}}_K \underline{\gamma_0^K \psi},$$

where the underline refers to the coefficient vector of the expansion in the basis Φ^q . Since $\underline{\mathbf{S}}_K$ is a symmetric matrix, the approximation of the bilinear form is also symmetric with respect to its arguments. Consequently, the approximated system matrix in the system of linear equations obtained by (24) is symmetric and the element matrices $\underline{\mathbf{S}}_K$ serve as local stiffness matrices in the setup process.

If both functions $\psi, \varphi \in \Psi_{h,\circ}^q$ are element basis functions, the property (5) is utilized. For $\psi = \psi_{K,i,j}$ and $\varphi = \psi_{K,k,\ell}$, we obtain

$$b(\psi_{K,i,j}, \psi_{K,k,\ell}) = a_K(\nabla \psi_{K,i,j}, \nabla \psi_{K,k,\ell})_{L_2(K)} = a_K(p_{K,i,j}, \psi_{K,k,\ell})_{L_2(K)},$$

where $p_{K,i,j} \in \mathcal{P}^{q-2}(K)$, see (4). The L_2 -scalar products are treated again with quadrature as in the previous situation for $(f, \varphi)_{L_2(\Omega)}$. If the functions ψ, φ belong to different elements, we just get zero, since the supports of them do not intersect.

4.4 Comments on the strategy

In Subsection 4.1, we already observed that in the case of a vanishing source term, i.e. $f = 0$, it is sufficient to seek the approximation $u_h \in V_h^q$ in the subspace $V_{h,\partial}^q$. This observation is confirmed by the decoupling of the Galerkin formulation. Because of $u_h = u_{h,\partial} + u_{h,\circ}$ with $u_{h,\partial} \in V_{h,\partial}^q$, and since the part $u_{h,\circ} \in V_{h,\circ}^q$ is uniquely defined by (25), we get $u_{h,\circ} = 0$ for $f = 0$ and thus $u_h = u_{h,\partial}$.

Furthermore, the property (23) and consequently the decoupling of the system is very attractive from the computational point of view. The global system of linear equations reduces to a system which only involves the degrees of freedom corresponding to node and edge basis functions. The unknowns for the element basis functions can be computed element-by-element in a preprocessing step. This is an advantage over the Virtual Element Method in [3]. This method has the same number of unknowns, but the system matrix does not decouple and thus, a larger system of linear equations has to be solved. Another advantage of the BEM-based FEM in this context is that the approximation u_h can be evaluated in every point inside of the domain with the help of the representation formula (21). The Virtual Element Method, however, needs some postprocessing for the evaluation in an arbitrary point.

In the case of a continuous varying diffusion coefficient in the model problem (1), it is possible to approximate the coefficient by a piecewise constant function.

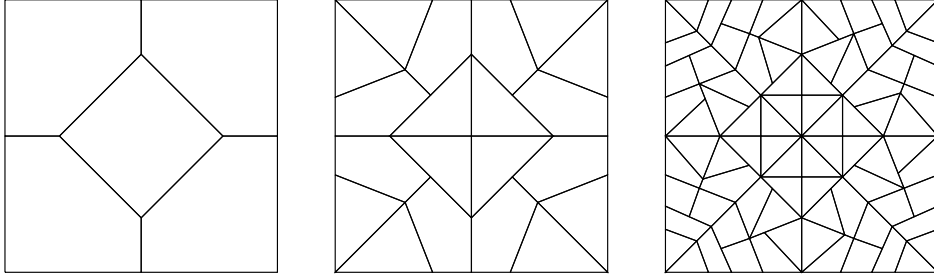


Figure 4: Initial mesh (left), refined mesh after two steps (middle), refined mesh after four steps (right)

Thus, the presented approximation of the Galerkin formulation in the BEM-based Finite Element Method is applicable. However, to obtain arbitrary order of convergence, this piecewise constant approximation is not sufficient. It is recommendable to approximate the diffusion coefficient by a smoother function. For a sufficient regular coefficient a , one can use its interpolation $\mathfrak{J}_h^{q-1}a$, for example. For a more detailed discussion and for implementation details, see [28]. The ideas given there can be generalized to $q > 2$ directly.

5 Numerical experiments

Finally, the theoretical results are verified by some computational experiments. For convenience, we utilize the same problems as in [28]. The underlying domain is the unit square, which is discretized by a sequence of polygonal meshes, see Figure 4.

Example 1. Consider the boundary value problem

$$\begin{aligned} -\Delta u &= f & \text{in } \Omega &= (0, 1)^2, \\ u &= 0 & \text{on } \Gamma, \end{aligned}$$

where f is chosen such that $u(x) = \sin(\pi x_1) \sin(\pi x_2)$ is the unique solution.

The first example demonstrates the BEM-based Finite Element Method with the full ansatz space V_h^q . According to the Theorems 2 and 3, we expect convergence of $\mathcal{O}(h^q)$ in the H^1 -norm and $\mathcal{O}(h^{q+1})$ in the L_2 -norm, respectively. This behaviour can be seen clearly in Figure 5.

Example 2. Consider the boundary value problem

$$\begin{aligned} -\Delta u &= 0 & \text{in } \Omega &= (0, 1)^2, \\ u &= g_D & \text{on } \Gamma, \end{aligned}$$

where g_D is chosen such that $u(x) = \exp(2\pi(x_1 - 0.3)) \cos(2\pi(x_2 - 0.3))$ is the unique solution.

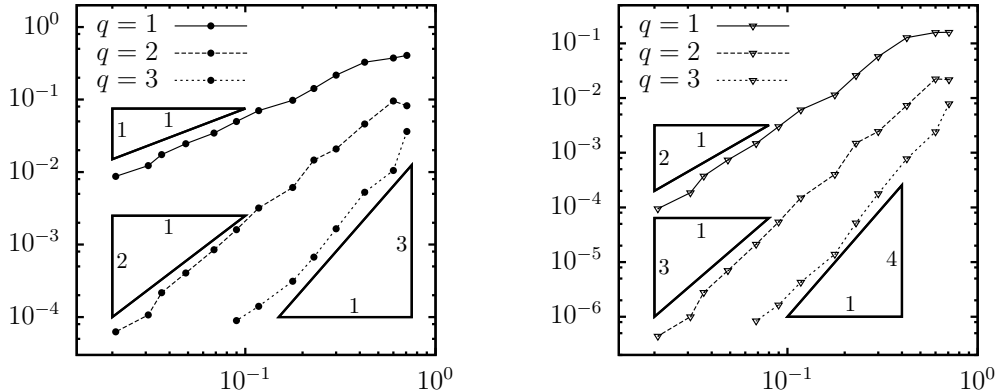


Figure 5: Relative error in H^1 -norm (left) and L_2 -norm (right) with respect to the mesh size h for Example 1 with ansatz space V_h^q

In the second example, we solve the Laplace problem with given Dirichlet data. Since the solution is obviously harmonic, the reduced Galerkin formulation is applied in the computations. Thus, only node and edge basis functions are used in the Finite Element Method. Although the ansatz space is reduced, we obtain optimal rates of convergence in the H^1 - as well as in the L_2 -norm, see Figure 6. These results are in accordance with the theoretical rates of Theorem 4.

6 Conclusion

We gave a rigorous construction of an H^1 -conforming approximation space which yields arbitrary order of convergence in a Finite Element Method on quite general meshes. It is constructed but not limited to the diffusion equation. We observed that only a subspace is needed for the approximation of piecewise harmonic functions. This reduces the computational effort and gives new insights into the BEM-based FEM.

Forthcoming research is intended to generalize and to apply the ideas of the BEM-based Finite Element Method to more general situations. For convection-diffusion problems, the construction of trial functions promises some stability properties. Furthermore, the topic of mixed formulations is under investigation and the first results are already published in [11].

References

- [1] R. A. Adams. *Sobolev Spaces*. Academic Press, 1975.

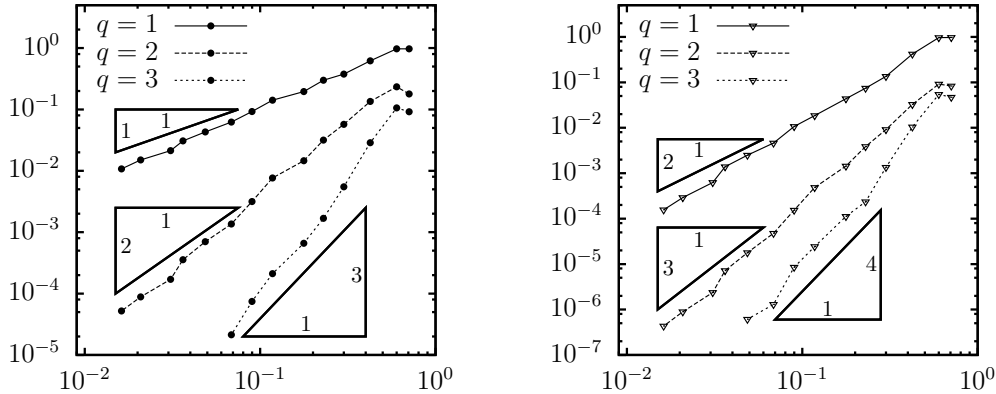


Figure 6: Relative error in H^1 -norm (left) and L_2 -norm (right) with respect to the mesh size h for Example 2 with the reduced ansatz space $V_{h,\partial}^q$

- [2] B. Ahmad, A. Alsaedi, F. Brezzi, L.D. Marini, and A. Russo. Equivalent projectors for virtual element methods. *Comput. Math. Appl.*, 66(3):376–391, 2013.
- [3] L. Beirão da Veiga, F. Brezzi, A. Cangiani, G. Manzini, L. D. Marini, and A. Russo. Basic principles of virtual element methods. *Math. Models Methods Appl. Sci.*, 23(01):199–214, 2013.
- [4] L. Beirão da Veiga, F. Brezzi, and L. Marini. Virtual elements for linear elasticity problems. *SIAM J. Numer. Anal.*, 51(2):794–812, 2013.
- [5] L. Beirão da Veiga, K. Lipnikov, and G. Manzini. Arbitrary-order nodal mimetic discretizations of elliptic problems on polygonal meshes. *SIAM J. Numer. Anal.*, 49(5):1737–1760, 2011.
- [6] D. Braess. *Finite Elements*. Cambridge University Press, Cambridge, third edition, 2007. Theory, fast solvers, and applications in elasticity theory, Translated from the German by Larry L. Schumaker.
- [7] S. C. Brenner and L. R. Scott. *The Mathematical Theory of Finite Element Methods*, volume 15 of *Texts in Applied Mathematics*. Springer, New York, second edition, 2002.
- [8] P. G. Ciarlet. *The Finite Element Method for Elliptic Problems*. North-Holland, Amsterdam, 1978.
- [9] D. Copeland, U. Langer, and D. Pusch. From the boundary element domain decomposition methods to local Trefftz finite element methods on polyhedral meshes. In *Domain decomposition methods in science and engineering XVIII*,

volume 70 of *Lect. Notes Comput. Sci. Eng.*, pages 315–322. Springer, Berlin Heidelberg, 2009.

- [10] D. M. Copeland. Boundary-element-based finite element methods for Helmholtz and Maxwell equations on general polyhedral meshes. *Int. J. Appl. Math. Comput. Sci.*, 5(1):60–73, 2009.
- [11] Y. Efendiev, J. Galvis, R. Lazarov, and S. Weißer. Mixed FEM for second order elliptic problems on polygonal meshes with BEM-based spaces. In *Large-Scale Scientific Computing*, Lecture Notes in Computer Science. Springer, Berlin Heidelberg. (to appear).
- [12] A. Gillette, A. Rand, and C. Bajaj. Error estimates for generalized barycentric interpolation. *Adv. Comput. Math.*, 37:417–439, 2012.
- [13] P. Grisvard. *Elliptic problems in nonsmooth domains*. Monographs and studies in mathematics. Pitman Advanced Pub. Program, 1985.
- [14] C. Hofreither. L_2 error estimates for a nonstandard finite element method on polyhedral meshes. *J. Numer. Math.*, 19(1):27–39, 2011.
- [15] C. Hofreither. *A Non-standard Finite Element Method using Boundary Integral Operators*. PhD thesis, Johannes Kepler University, Linz, Austria, December 2012.
- [16] C. Hofreither, U. Langer, and C. Pechstein. Analysis of a non-standard finite element method based on boundary integral operators. *Electron. Trans. Numer. Anal.*, 37:413–436, 2010.
- [17] C. Hofreither, U. Langer, and C. Pechstein. A non-standard finite element method for convection-diffusion-reaction problems on polyhedral meshes. *AIP Conference Proceedings*, 1404(1):397–404, 2011.
- [18] P. Jamet. Estimations d’erreur pour des éléments finis droits presque dégénérés. *RAIRO Anal. Numér.*, 10(R-1):43–60, 1976.
- [19] P. Joshi, M. Meyer, T. DeRose, B. Green, and T. Sanocki. Harmonic coordinates for character articulation. *ACM Trans. Graph.*, 26(3):71.1–71.9, 2007.
- [20] V. V. Karachik and N. A. Antropova. On the Solution of the Inhomogeneous Polyharmonic Equation and the Inhomogeneous Helmholtz Equation. *Differential Equations*, 46(3):387–399, 2010.
- [21] S. Martin, P. Kaufmann, M. Botsch, M. Wicke, and M. Gross. Polyhedral finite elements using harmonic basis functions. *Comput. Graph. Forum*, 27(5):1521–1529, 2008.

- [22] W. C. H. McLean. *Strongly elliptic systems and boundary integral equations*. Cambridge University Press, Cambridge, 2000.
- [23] S. E. Mousavi and N. Sukumar. Numerical integration of polynomials and discontinuous functions on irregular convex polygons and polyhedrons. *Comput. Mech.*, 47:535–554, 2011.
- [24] C. Pechstein and C. Hofreither. A rigorous error analysis of coupled FEM-BEM problems with arbitrary many subdomains. *Lecture Notes in Applied and Computational Mechanics*, 66:109–132, 2013.
- [25] A. Rand, A. Gillette, and C. Bajaj. Quadratic serendipity finite elements on polygons using generalized barycentric coordinates. *Math. Comput.* (to appear).
- [26] S. Rjasanow and O. Steinbach. *The fast solution of boundary integral equations*. Mathematical and analytical techniques with applications to engineering. Springer, 2007.
- [27] S. Rjasanow and S. Weißer. FEM with Trefftz trial functions on polyhedral elements. Technical report, Fachrichtung 6.1 – Mathematik, Universität des Saarlandes, 2012.
- [28] S. Rjasanow and S. Weißer. Higher order BEM-based FEM on polygonal meshes. *SIAM J. Numer. Anal.*, 50(5):2357–2378, 2012.
- [29] O. Steinbach. *Numerical approximation methods for elliptic boundary value problems: finite and boundary elements*. Springer, New York, 2007.
- [30] A. Tabarraei and N. Sukumar. Application of polygonal finite elements in linear elasticity. *Int. J. Comput. Methods*, 3(4):503–520, 2006.
- [31] S. Weißer. Residual error estimate for BEM-based FEM on polygonal meshes. *Numer. Math.*, 118(4):765–788, 2011.
- [32] S. Weißer. *Finite Element Methods with local Trefftz trial functions*. PhD thesis, Universität des Saarlandes, Saarbrücken, Germany, September 2012.